Citation: Tsang, S.W.R., Lindsay, J.M., Coco, G. et al. The heating of substrates beneath basaltic lava flows. Bull Volcanol 81, 68 (2019). https://doi.org/10.1007/s00445-019-1320-y

The heating of substrates beneath basaltic lava flows

Sophia W. R. Tsang*

School of Environment, University of Auckland, Auckland, New Zealand

s.tsang@auckland.ac.nz, +64 21 2614438, ORCID: 0000-0002-0156-4495

Jan M. Lindsay

School of Environment, University of Auckland, Auckland, New Zealand

j.lindsay@auckland.ac.nz

Giovanni Coco

School of Environment, University of Auckland, Auckland, New Zealand

g.coco@auckland.ac.nz

Robert Wysocki

School of Art, Syracuse University, Syracuse, NY, USA

rjwysock@syr.edu

Geoffrey A. Lerner

School of Environment, University of Auckland, Auckland, New Zealand

g.lerner@auckland.ac.nz

Erika Rader

Department of Geological Sciences, University of Idaho, Moscow, ID, USA, formerly

Planetary Systems Branch, NASA Ames Research Center, Mountain View, CA, USA

erader@uidaho.edu

Gillian M. Turner

School of Chemical and Physical Sciences, Victoria University of Wellington, Wellington, New Zealand
Gillian.turner@vuw.ac.nz
Ben Kennedy
Department of Geological Sciences, University of Canterbury, Christchurch, New Zealand
ben.kennedy@canterbury.ac.nz

Abstract

As populations around volcanoes grow, the potential for society to be impacted by lava flows is increasing. While lava flows are known to ignite, bulldoze, and/or bury structures, little is known about potential impacts to buried infrastructure. We measure temperature profiles below molten rock to constrain a heat transfer model. Thermomagnetic and palaeomagnetic measurements on soil samples from beneath a 2014 Hawaiian lava flow are then used to verify the model. Finally, we illustrate the model's utility in lava flow hazard assessments by modelling a hypothetical lava flow active for four weeks in Auckland (New Zealand). The modelling predicts the upper 1.7 m of dry soil would exceed 100°C after one week, and the upper 3.8 m of soil would exceed 100°C after four weeks. Determining the depth profile of substrate heating has important implications for planning and preparedness (e.g. siting buried infrastructure), volcanic impact and risk assessments, and decision-making before and during lava flow crises (e.g. mitigation measures to be employed).

Keywords

Thermal modelling, lava flow hazard, palaeomagnetism, analogue experiment, pāhoehoe, infrastructure impact

Introduction

The substrate beneath lava flows and around intrusions is frequently discoloured and/or desiccated, indicating significant heat transfer from the molten rock into its surroundings (e.g. Lovering 1955; Bell et al. 1993; Baker et al. 2015). Recent eruptions, such as on Fogo, Cape Verde in 2014–2015 and in Hawaii in 2014 and 2018, illustrate the impact of lava flows on communities (Jenkins et al. 2017; Harris 2015) and infrastructure (Patrick et al. 2017; Big Island Now 2018 May 6). Heat transferred into the ground can affect the operation of buried infrastructure due to exposure to high temperatures from overriding lava flows. Indeed, infrastructure providers have expressed concern about potential impacts to their assets, including water and electricity networks (Hawaiian Electric Light Company (HELCO) *pers. comm.* (07/04/2017); Hawai'i County Department of Water Supply (DWS) *pers. comm.* (19/04/2017)). Infrastructure providers thus require temperature profile estimates below the flow to make decisions (HELCO *pers. comm.* (07/04/2017); Hawai'i County DWS *pers. comm.* (19/04/2017)). Furthermore, excessive heat has the potential to destroy microbial and plant life (e.g. Blong 1984; Goodhue and Clayton 2010; Rumpf et al. 2013). Despite the range of potential temperature-related subterranean impacts, the amount of heat transferred by a lava flow into the substrate and the rate at which it is transferred have not been well constrained.

Temperature distributions surrounding intrusive features have been numerically modelled using the Fourier heat conduction equation for nearly a century (Lovering 1935). Early work modelled instantaneously emplaced magma into dry country rock and showed that the release of latent heat of crystallisation can increase the magma-country rock contact temperature by up to 100°C and double its cooling duration (Jaeger 1957; Reilly 1958). Later work determined that the country rock's temperature profile is primarily determined by the ratio of the magma's solidification to intrusion temperatures (Delaney and Pollard 1982). Computers allow for more complex calculations, such as those that consider temperature-dependent properties that can span multiple orders of magnitude (Delaney 1987; Hort 1997). Using such approaches, a modelled temperature profile surrounding a sill in Idaho revealed that convection dominates the heat transfer in waterlogged soil (Baker et al. 2015). Previous work shows that sediments under lava flows can experience higher temperatures than sediments surrounding intrusive features at equal distances with other variables being similar

(Wilson 1962), suggesting that intrusive heat transfer studies cannot be applied accurately to lava flows. Additionally, the scarcity of experimental and field data from beneath lava flows necessitates exploring a numerical modelling approach.

Previous work on thermal budgets of lava flows has primarily focused on the upper half of the flows (e.g Ishihara et al. 1989; Patrick et al. 2004; Keszthelyi et al. 2005). Field data shows that convection in the air above a lava flow is the dominant cooling mechanism when the lava flow is below 520°C and that free convection in the air can be as effective as forced convection when the lava is below 400°C and wind speeds are low (Keszthelyi et al. 2005). Numerical modelling of the 1997 Okmok lava flow revealed that either convection or radiation dominates cooling, depending on meteorological conditions (Patrick et al. 2004). Many models also acknowledge that heat must also be transferred into the ground (Ishihara et al. 1989; Patrick et al. 2004) although they do not model the ground temperatures. There have been attempts to measure the basal temperatures of lava flows, but the few field datasets available are too short to constrain modelling. The longest continuous record is 400 hours, with temperatures collected in the crust of the flow and at 10 and 20 cm depth from the crust (Hon et al. 1993; Keszthelyi 1995; Keszthelyi and Denlinger 1996). These surface and interior temperature records allow for inferences on cooling and the evolution of the flow’s thermal history. However, only Keszthelyi (1995) presents direct measurements of temperature beneath an advancing lava flow, and those datasets range from only 2 to 8 minutes long. Laboratory datasets are all shorter (Edwards et al. 2003) and have only been used to model temperature gradients inside lava flows, not in the country rock. Previous lunar lava flow-regolith heat transfer modelling (Rumpf 2015) has not been constrained by field data and is not applicable to terrestrial settings since different atmospheric and gravity conditions will affect convective heat transfer rates. Most lava-substrate heat transfer modelling has focused on thermal erosion processes, and suggests significant heat transfer must occur to initiate thermal erosion (Bussey et al. 1995; 1997). Most recently, Fagents and Greeley (2001) used computational fluid dynamics modelling to determine that the ideal conditions for thermal erosion by a basaltic lava flow are uncommon on Earth, although they are potentially more common on other planetary bodies (Fagents and Greeley 2001) and in lava tubes (e.g. Greeley et al. 1998; Kauahikaua et al. 1998; Kerr 2009).

This paper focuses on lava-substrate heat transfer during the period before the lava-substrate contact reaches the substrate's solidus (i.e. the time domain before thermal erosion could commence). We present a lava flow-substrate heat transfer model constrained with molten rock experiments that simulate pāhoehoe lava flows. Furthermore, the model is verified through magnetic and palaeomagnetic measurements on soil samples heated by overlain past lava flows. Heating to several hundred degrees is known to enhance the ferrimagnetic mineralogy of soils (Evans and Heller, 2003). In addition, during the subsequent cooling in the ambient geomagnetic field, a thermoremanent magnetisation (TRM) is imparted to the soil in the interval of its magnetic blocking temperature spectrum below the peak temperature reached (e.g. Evans and Heller, 2003; Butler, 2004; Tauxe, 2010). Thus, the stability and intensity of the magnetic field can be used to infer the relative extent to which materials have been heated. The utility of the heat transfer model is then demonstrated by modelling the temperature profile under a hypothetical pāhoehoe flow.

Methods

Molten Rock Experiments

We undertook molten rock experiments at the Syracuse University Lava Project (http://lavaproject.syr.edu/) by pouring basaltic material into steel pipes filled with substrate material(s) and collecting temperature data using k-type thermocouples and a FLIR T300 (spatial resolution: 1.36 mrad; thermal image size: 320 pixels by 240 pixels) thermal camera. Molten rock and soil temperatures were collected once per minute, in the centre of the substrates, every 20 cm below the molten rock-substrate contact. Eight Omega data loggers (accuracy: within 1% of measured temperature + 0.7°C) took temperature measurements every minute until two conditions were met: 1) the molten rock-substrate contact temperature dropped below 200°C and 2) all the soil temperatures were decreasing. The thermal camera was used to take approximately level, still images of the molten rock from 2–5 m away.

At the Lava Project, a natural gas Gasmac tilt-furnace has been repurposed to melt a meta-basalt in the greenschist facies sourced from the Chengwatana Volcanics (Lev et al. 2012; Dietterich et al. 2015; Rumpf et al. 2018) in the Midwestern USA; see Wirth et al. (1997) for bulk geochemistry. In our experiments, we heated the metabasaltic material to 1300°C for at least four hours to ensure a uniform temperature and to minimise the volatile content in the resulting molten rock (Dietterich et al. 2015). The tilt-furnace was positioned to pour the molten rock into a steel pipe, which was positioned in a sand pit under the furnace's spout (Fig. 1b).

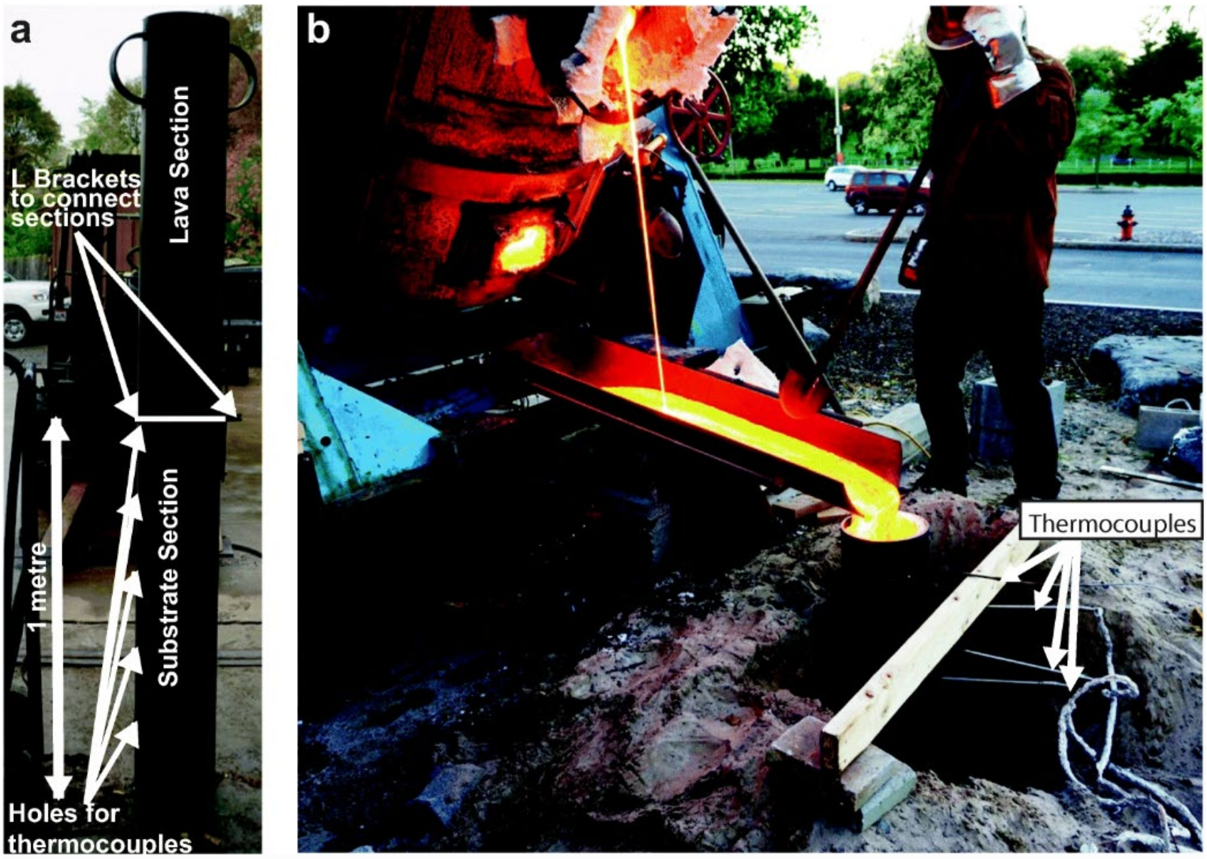

Fig. 1 a) Two pipe sections created to simulate a 1-metre thick lava flow. The lava section of each pipe was lined with ceramic blanket to minimise the heat loss (Fig. 2). b) Pipe for a 10 cm thick lava experiment positioned in the sand pit. Note the position of the thermocouples.

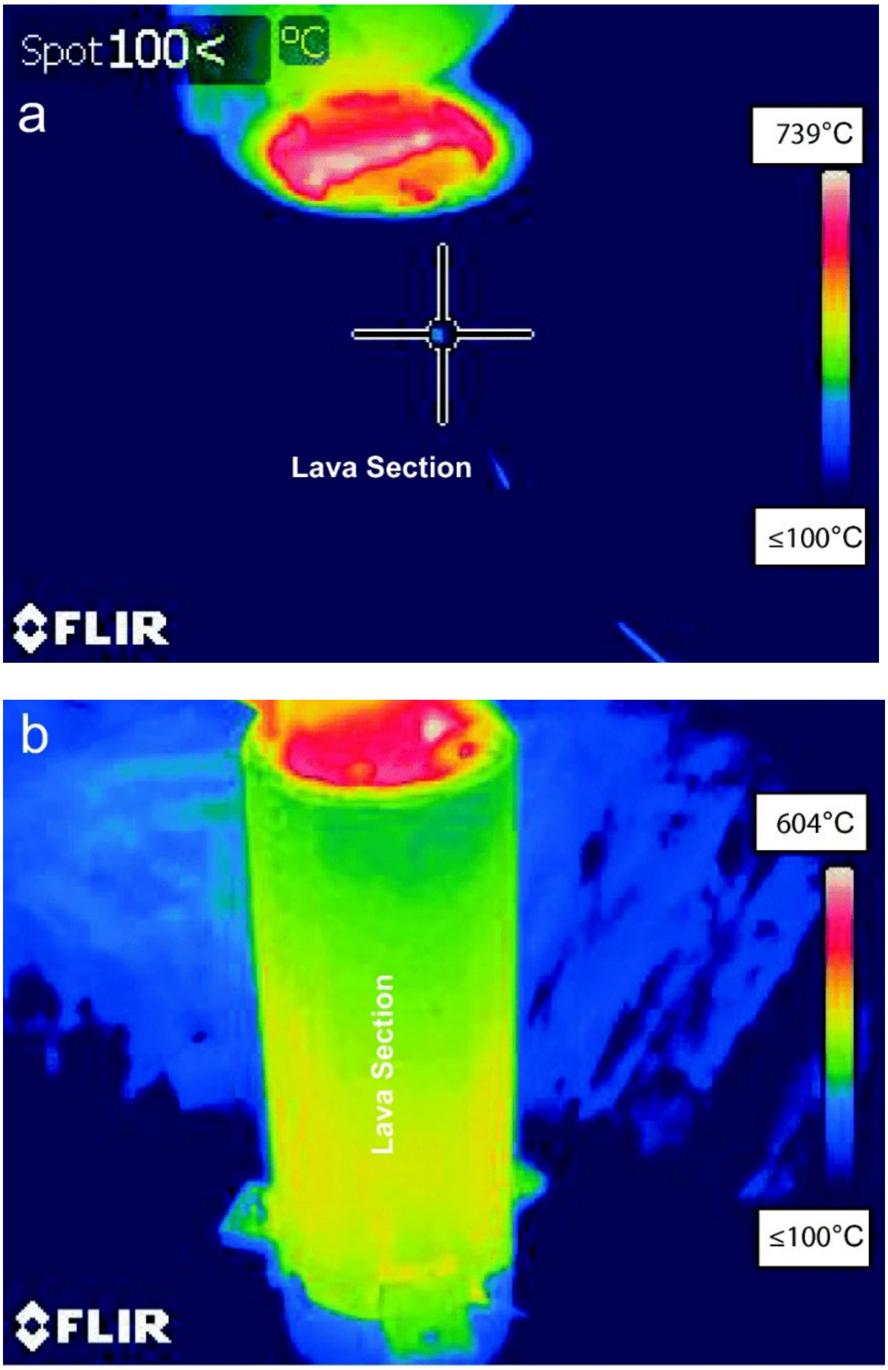

Fig. 2 a) Outside of pipe with 10 cm of lava inside. When the image was taken, the temperature at the contact between the soil and the lava was 896.3°C while the upper crust was 739°C. The temperature of the pipe containing the lava was less than 100°C. b) Outside of pipe with 50 cm of lava inside. The soil-lava contact temperature was 1016°C while the upper crust was 604°C. The outside of the pipe holding the lava was 229°C.

We conducted four experiment types to determine temperature profiles beneath molten rock flows in substrates consisting of dry soil, wet soil, soil under footpaths, and soil under roads. Topsoil sourced from the local garden store was used in all experiments. The footpath and road cross-sections were constructed according to Auckland (New Zealand) standards (Auckland Transport 2013a; Auckland Transport 2013b). We used a 10-cm-thick layer of concrete and an 8-cm-thick layer of granular base on top of dry soil in the footpath experiments. In the road experiments, the concrete and granular base were replaced with a 3-cm layer of bitumen and a 35-cm-thick sub-base layer. For dry soil and wet soil experiments, we tested three molten rock thicknesses—10 cm, 50 cm, and 100 cm—three times each. For footpath and road experiments, we tested a molten rock thickness of 50 cm twice each. All experimental data are included in Online Resource 1.

We designed and fabricated a series of steel pipes 20.3 cm in diameter for the experiments (Fig. 1a). The pipe diameter ensured the temperature measurements could be taken at least 10 cm from the edge of the pipe (Fig. 2). This diameter was selected to balance practical concerns (i.e. thermocouple could reach centre of pipe and filled pipes could be moved) and maximise the distance from the pipe walls to the measurement locations. The pipes were lined with compacted Fiberfrax® (2 cm thick prior to compaction) to insulate the molten rock and prevent heat loss to the pipe walls. Each experiment consisted of two sections of pipe: an upper lava pipe and a lower substrate pipe that were bolted together using welded steel L-brackets (Fig. 1a). The physical separation of several millimeters afforded by the brackets between the sections limited the heat transferred from the upper pipe (containing the molten rock) to the substrate below via the lower pipe (Fig. 2).

We produced the lower sections in two lengths (70 cm and 1 m long) to allow for a range of different substrate thicknesses. We drilled holes into the side of each pipe every 20 cm to enable thermocouples to be inserted (Fig. 1b). Thermocouple placement was determined by the expected range of heating and the number of available data loggers. We made the upper sections in three sizes (10 cm, 50 cm, and 100 cm) to allow for different molten rock thicknesses. We then filled the lower sections with substrates that are commonly found in urban areas. We packed the topsoil into the bottom steel pipes until the bulk density was 1400 kg/m^3, approximately the same as the measured soil density in Auckland, New Zealand (Atlas Concrete Ltd, 2011; Rifareal, 2011). For the soil experiments, we filled the pipes to the top with soil. For the dry soil experiments, we poured the topsoil onto a dry surface inside the laboratory near two floor furnaces and allowed it to desiccate for at least 12 hours before filling the pipes. For the wet soil experiments, we filled the bottom steel pipes with topsoil. We then added water to the pipe until the soil was fully saturated to create a wet soil endmember. The resulting bulk density was approximately 1800 kg/m^3. For the footpath and road experiments, we filled the bottom pipes with 52 cm and 32 cm of soil, respectively, and then covered the soil with the surficial covering being tested in that experiment. For the footpath experiment, we added an 8-cm-thick layer of gravel equivalent in diameter to granular sub-base on top of the soil (mean grain size: 1.6 cm (Rumpf et al. 2018)). Granular sub-base is defined as sand, gravel, crushed rock, slag, or other durable material that is densely graded and has at least 50% coarse material (the latter to promote drainage, among other characteristics). Coarse material is defined as material with a maximum grain size of 50 mm and with less than 8% fine material (less than 0.075 mm; Federal Highway Administration Research and Technology 2016). We then placed a 10-cm-thick slab of concrete on top of the sub-base. For the road experiment, we added a 35-cm layer of gravel, equivalent in size to granular base, on top of the compacted soil (mean grain size: 2.9 cm (Rumpf et al. 2018)). Granular base is similar to granular sub-base except it consists of finer materials (nominal maximum size of up to 100 mm with less than 12% fine material; Federal Highway Administration Research and Technology 2016). Finally, we added a 3-cm layer of commercial grade asphalt patch (bitumen).

The pipes were then placed in the sand pit below the Gasmac tilt-furnace (Fig. 1b), and the tilt-furnace was rotated to pour molten rock into the pipe until the molten rock level was flush with the top of the pipe (Fig. 1b). Because the molten rock began cooling as soon as it left the furnace, these pours could be considered equivalent to when a lava flow is no longer supplied lava, i.e. is stagnant and cooling. It is thus henceforth referred to as the “cooling-only phase”.

Once the molten rock had formed a stable crust, we removed the pipes from the sand pit and placed them in a more stable location. The thermocouple records showed some anomalous data in which the temperatures recorded changed more rapidly than physically possible. These anomalous data were all generated while the pipes were being moved, which typically occurred within the first half hour of the experiment (Online Resource 1). These data points remain in the data (Online Resource 1) although were ignored when constraining the heat transfer model.

In every experiment, we placed a k-type thermocouple in the centre of the pipe at the contact between the molten rock and the soil, bitumen, or concrete. We also inserted thermocouples into the pipes every 20 cm below the molten rock-substrate contact. The initial surface temperature of the molten rock as it was poured into the pipes was measured by the thermal camera (Fig. 2) and ranged from 1018°C to 893°C (Online Resource 2). Videos of the molten rock pours are included in Online Resources 3 through 11.

Magnetic and palaeomagnetic analyses

Soil samples were collected from depths of 3–5, 8–10, 13–15, and 23–25 cm in the substrate beneath a Kīlauea Volcano, Hawaii, lava flow named the June 27th Lava Flow (sample location: 19.4946°N 154.954°W; lava flow active: 2014-2015). A control sample was also collected from material that had not been covered by lava. Standard 6.9 cm^3 cubic plastic boxes were used for sample collection, with the vertical direction being recorded. All samples originated from a manmade soil berm constructed from poorly-sorted soil sourced locally, i.e. derived from basaltic lava flows.

Ideally, to obtain a palaeomagnetic estimate of the maximum temperature reached, it is necessary to progressively demagnetise a sample by incrementally heating and cooling it in a magnetic field-free environment and measuring the consequent loss of magnetisation. By repeating this process to progressively higher temperatures, the unblocking temperature spectrum of the natural remanent magnetisation (in this case a TRM) is recovered. Assuming reciprocity of blocking and unblocking, the maximum temperature reached in the magnetisation process is estimated as the highest unblocking temperature (Paterson et al. 2010). This method is frequently used to estimate emplacement temperatures of both clasts and matrix material in pyroclastic flows (Kent et al. 1981; Turner et al. 2018; Lerner et al. 2019). In the present study it was impractical to use thermal demagnetisation as described above since the samples are unconsolidated and in plastic boxes. We therefore decided to trial progressive demagnetisation by the analogous alternating magnetic field (AF) technique, which is carried out at room temperature. This method involves studying the coercivity spectrum of a sample as opposed to the blocking temperature spectrum (As and Zijderveld 1958). Analyses were carried out at the Palaeomagentism Laboratory at Victoria University of Wellington, New Zealand.

A Molspin AF demagnetiser was used to carry out the AF demagnetization. The peak alternating field was incremented in steps of 2.5 mT until the remaining remanence was less than 5% of the original. After each step, the remanence was measured using an Agico JR-6 spinner magnetometer (sensitivity: 2×10^{-6} A/m). Visualisation and principal component analysis of the data were carried out using the Remasoft software package (Chadima and Hrouda 2006). After removing the samples from their plastic boxes, we recorded the variation of magnetic susceptibility from room temperature to 700°C (this being above the Curie temperatures of all naturally occurring ferro/imagnetic minerals), and back to room temperature using a Bartington Instruments MS2 magnetic susceptibility system and furnace. Magnetic susceptibility depends on the magnetic mineral(s) present in a sample and their concentration, being in general dominated by ferri- or ferro- magnetic minerals such as magnetite, maghaemite and haematite (Thompson et al. 1980; Evan and Heller 2003). Monitoring the variation of magnetic susceptibility with temperature reveals thermally-induced changes in the magnetic mineralogy and the Curie temperature(s) of constituent ferri- or ferro-magnetic minerals.

Heat transfer modelling

We used ANSYS, Inc.'s (https://www.ansys.com/) Mechanical ANSYS Parametric Design Language (MAPDL) software package to simulate the heat transfer between lava flows and the underlying substrates. The MAPDL software package uses the strong formulation of the partial differential equations describing heat transfer (ANSYS 2017). Programs by ANSYS are commonly used by stakeholders, such as the engineering departments at utility providers (e.g. Transpower in New Zealand), which allow our results to be integrated into stakeholder models easily. The geometry of the model and heat transfer across boundaries is shown in Fig. 3. Heat is transferred in both directions across all boundaries. In a given material, conduction was the only heat transfer mechanism considered. We conducted a mesh refinement study to determine the uncertainty arising from the discretisation of the partial differential equations. The grid convergence index was 0.015% while the approximate relative error and extrapolated relative error were 0.220% and 0.012%, respectively. Other uncertainties include measurement error of the material properties and heat transfer mechanisms not considered by the model.

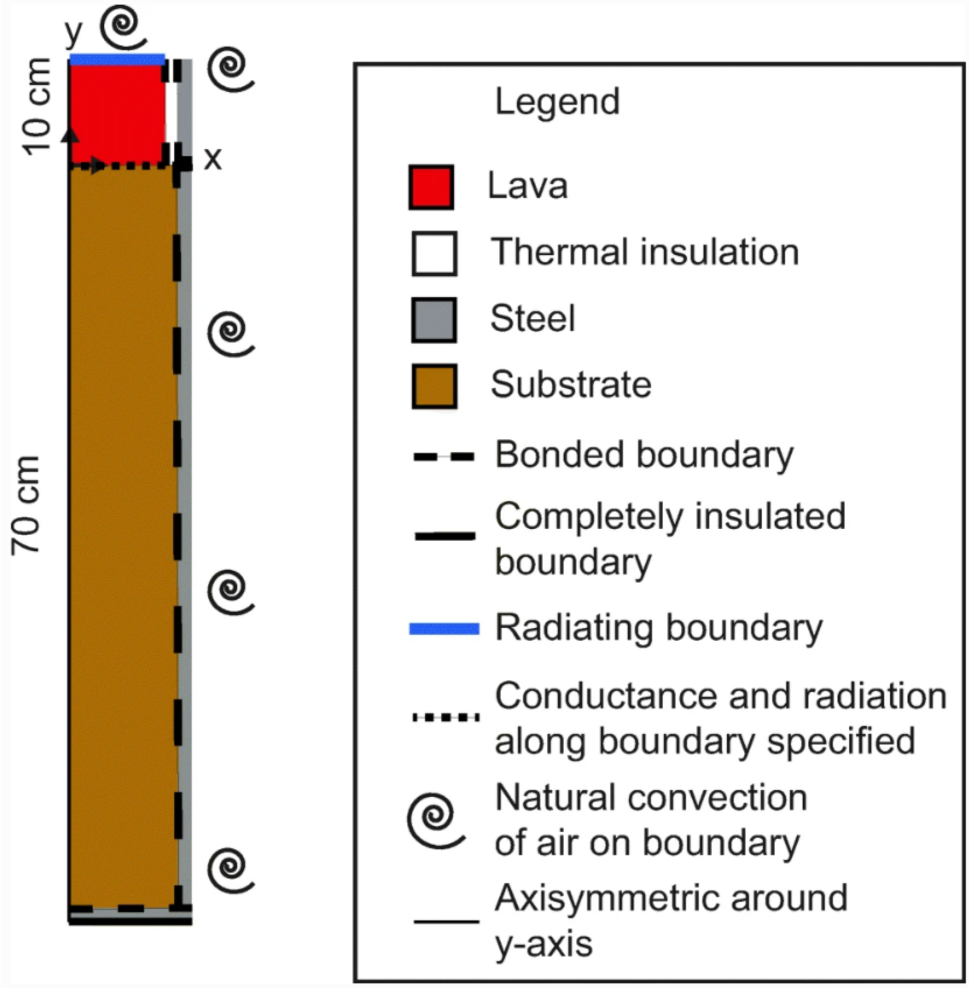

Fig. 3 Schematic diagram of 10 cm flow experiment used for heat transfer modelling.

The data from our laboratory molten rock experiments and Auckland soils guided the modelling of the cooling-only phase. We "filled" the bottom sections of the model with soil that had properties similar to the topsoil used at the Lava Project and the measured properties of Auckland soils (Tables 1, 2, and 3; Taihan New Zealand Ltd 2010; Rifareal 2011). The thermal properties of the simulated steel and insulation were sourced from industrial material data sheets (Tables 1 and 2; Lide 2005; Bergman et al. 2011; Zicar Ceramics 2016). The natural convection of air at the outer boundaries of the pipes was calculated by MPADL using the ambient temperatures when the laboratory experiments were run (Table 1). We set the initial temperature of the lava to match the lava temperature measured by the thermal camera (Online Resource 2). The thermal properties of the lava were initially set to match those used by Patrick et al. (2004) (Table 1) in their modelling of the 1997 Okmok (Alaska, USA) lava flow. The properties of the lava and the lava-soil contact were varied until the modelled temperatures were within 10% of the temperature and time of the experimental data. We were unable to remove the effects of the ambient temperature (i.e. to attribute a portion of the temperature changes measured to ambient temperature changes). To be able to do so, a sub-hourly dataset of ambient temperatures that matched our initial measured temperatures would be required. Such data could not be found within 10 km of the experimental location. The input properties used to recreate our laboratory data are displayed in Tables 1, 2, and 3. We considered heat transfer by conduction in the system, natural convection of air at the boundaries of the system, and radiation both at internal material boundaries and at the upper lava crust. We initially tested how the release of the latent heat of crystallisation affected soil temperatures by adding a heat generation source to the lava nodes when their temperature was 1050°C. Since the effect was minimal, subsequent tests did not include this heat source. This is probably because of the small lava volume being simulated: the heat source did not represent a large increase in the overall thermal budget. Other phase transitions (e.g. water vaporising) were not modelled. Additionally, ambient temperatures were treated as constant, although these could be varied in future modelling if ambient temperatures fluctuated significantly.

The palaeotemperatures recorded in the soils under lava flows reflect the maximum temperature reached under the lava flow during both the warming and cooling phases of the flow. Thus, we altered the initial cooling model to simulate the heat transfer while the lava flow is still flowing (i.e. being supplied with new material), creating a flowing phase model. To simulate this time domain, we held the lava temperature constant, similar to Fagents and Greeley (2001). In order to model a lava flow, we created a combined model by running the flowing model and providing the resulting temperature profile to the cooling model as initial conditions. No cooling was applied to the vertical surfaces of the lava and soil as these are artificial boundaries in the model. In a lava flow, these boundaries would be insulated by surrounding lava and soil, respectively.

Table 1 Input parameters for ANSYS MAPDL heat transfer modelling

Temperature in Celsius*	127	227	327	427	527	627	727	827	927	1027
Lava thermal conductivity (k_{lava}) [W/(mC)]**	7.5	6.5	6.4	6.3	5.5	4.8	3.5	2.4	2.23	2.2
Lava specific heat ($C_{p,lava}$) [J/(kgC)]*	520	600	680	710	735	1000	1100	1100	1100	1100
Lava density (ρ_{lava}) [kg/m^3] (Patrick et al. 2004)	2600									
Lava emissivity (ε_{lava}) (Patrick et al. 2004)	0.95									
Soil density (ρ_{soil}) [kg/m^3] (Taihan New Zealand Ltd 2010; Atlas Concrete Ltd 2011; Rifareal 2011)	1437.9									
Steel specific heat ($C_{p,steel}$) [J/(kgC)] (Lide 2005)	434									
Steel density (ρ_{steel}) [kg/m^3] (Lide 2005)	7900									
Insulation specific heat ($C_{p,insulation}$) [J/(kgC)] (Zicar Ceramics 2016)	1047									
Insulation density ($\rho_{insulation}$) [kg/m^3] (Zicar Ceramics 2016)	35									
Contact pair conductance [W/(m^{2}C)]*	6.5 (lava-soil)					1.5 (insulation-soil)				
Convection (h) [W/(m^{2}C)] *calculated*	8.41 (top)					2.0 (side)				
Mesh size [m] *selected by researchers*	0.01									
Lava temperature (T_{lava}) [°C] *measured*	800–1150									
Ambient temperature (T_{amb}) [°C] *measured*	Varied from 15 to 28 during experimental data collection period									

*Ansys MAPDL interpolates the properties between the temperatures provided
**Parameter varied to fit heat transfer model to experimental data

Table 2 Steel temperature-dependent input parameter for ANSYS MAPDL heat transfer modelling

Temperature in Celsius	315	540	760	980	1200
Steel thermal conductivity (k_{steel}) [W/(mC)]	0.10	0.09	0.13	0.17	0.23

Table 3 Input parameters for ANSYS MAPDL heat transfer modelling that changed based on whether the simulated soil was dry or wet

Model	**Dry**	**Wet**	
Temperature in Celsius	–	20	80
Soil thermal conductivity (k_{soil}) [W/(mC)]	0.75	1.5	2.8
Soil specific heat ($C_{p,soil}$) [J/(kgC)]	425	450	325

Results

Laboratory molten rock experiments

In all the experiments, the temperature at the molten rock-substrate contact rose to within 310°C of the molten rock temperature, although the difference between the contact and molten rock temperatures was often less. In one experiment, the temperature difference was less than 3°C. After, the molten rock-substrate contact temperature gradually fell to ambient temperature (varying between 16°C and 28°C depending on when the experiment was conducted), roughly following Newton's Law of Cooling (e.g. Adams and Rogers 1973; Arpaci et al. 2000; Holman 2010).

In the suite of soil experiments, the maximum soil temperatures measured 20 cm under the molten rock were less than 100°C (Online Resource 12). The maximum temperature reached at 20 cm was 73.8°C at 2.25 hours under 100 cm of molten rock and remained within a degree of this value for half an hour (Fig. 4). In comparison, the maximum temperature reached at 20 cm under 10 cm of molten rock was 47.5°C, reached after 3.2 hours. It remained within a degree of this for 0.6 hours. The soil temperature at 60 cm did not change due to the presence of molten rock in 9 of the 13 experiments. Indeed, at this distance, diurnal ambient temperature changes could be discerned (e.g. 60 cm below 10 cm of molten rock in Fig. 4a). There were a couple of notable differences between the wet and dry soil experiments. First, steam escaped the lower pipe in the beginning of the wet experiments. Second, the temperatures in the wet soil under the flows were up to 78°C higher in corresponding dry soil experiments at 20 cm. The temperature differences were most apparent at 20 cm below the molten rock-soil contact although they could also be discerned at 40 cm. The temperature difference at 40 cm was up to 9°C.

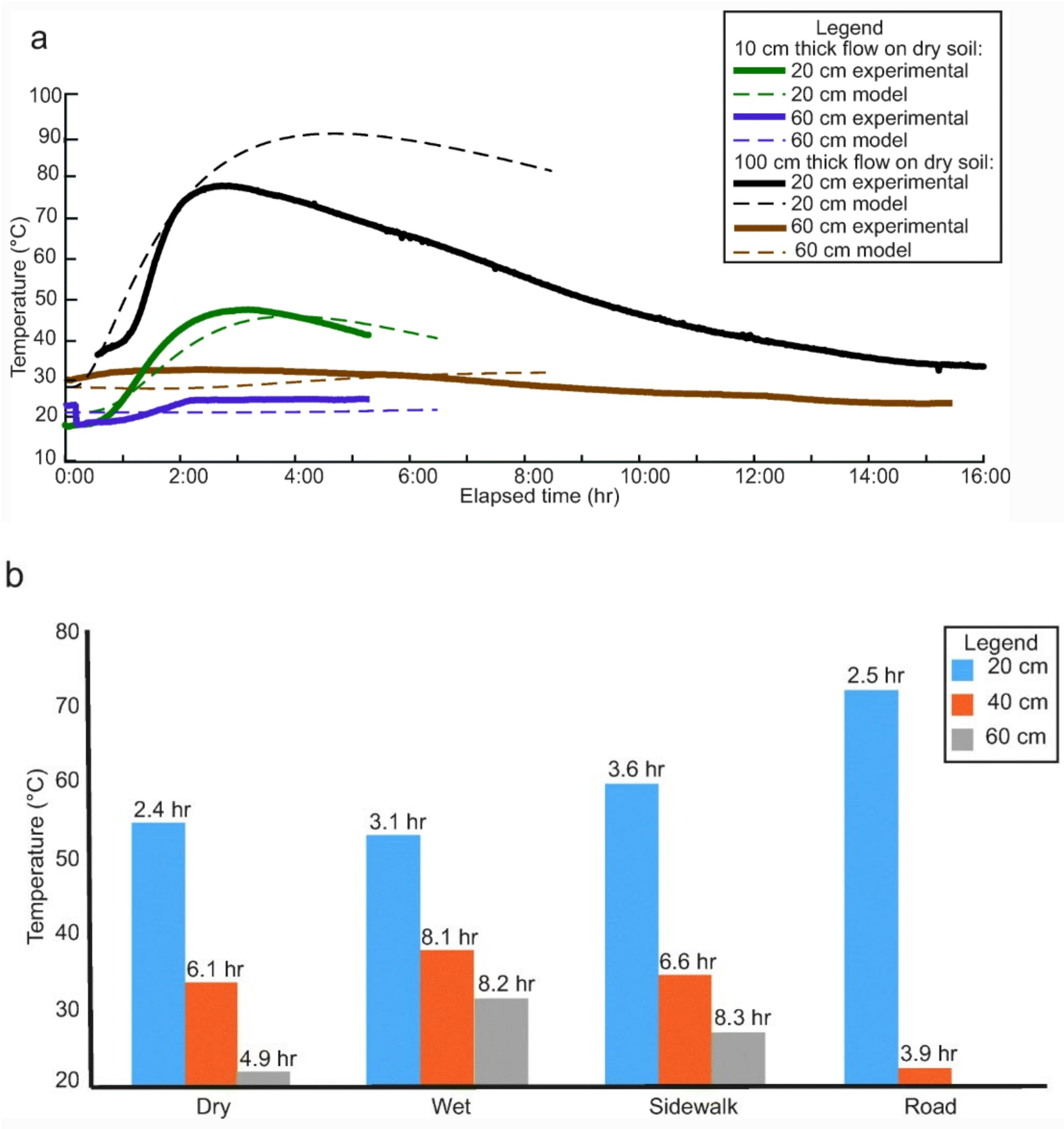

Fig. 4 a) Example time series graph showing the dry soil experimental and model temperatures at 20 cm and 60 cm deep for 10 cm and 100 cm thick molten rock experiments plotted over elapsed time. b) Example bar graph comparing the maximum temperatures reached in 50 cm thick molten rock experiments. The number above each bar indicates the elapsed time in hours for the soil at the given depth to reach the plotted temperature. A bar is not shown for 60 cm under the road as the temperature never increased, and both the ambient and measured temperatures were continually falling.

The second suite of molten rock experiments was set up to simulate 50 cm thick flows over urban ground coverings (i.e. footpaths and roads; Fig. 4b). The results from this suite of experiments differed from the soil experiments in a few key ways. First, the temperature of the granular base at 20 cm beneath the road covering peaked at 269.5°C at the beginning of the experiment. The substrate at 20 cm then cooled to 43°C after 1.25 hours before following a heating and cooling trend similar to the other experiments (Online Resource 1). Maximum temperatures reached at 20 cm in the dry soil, wet soil, and footpath experiments were all similar, ranging between 53°C and 59°C; the maximum temperature under the road at 20 cm was 71.8°C. This temperature was attained after 4.7 hours and was steady (within one degree) for 15 minutes. Additionally, green-tinged smoke was emitted as the lava came into contact with the bitumen, corresponding in time to the initially high temperatures. The uppermost granular base, naturally light gray, was stained black by dripping bitumen. The temperature spike was not measured below 20 cm in the road experiment. Finally, the substrates in the ground covering experiments took longer to heat and cool than in the dry soil experiments with the same molten rock thickness, indicated by the numbers at the top of each bar in Fig. 4b, despite ultimately displaying similar maximum temperatures. The time it takes the soil to reach the maximum temperatures is greatly dependent on the substrates' properties especially their thermal conductivities, which vary substantially.

Palaeomagnetic analysis

To verify the heat transfer model constrained by the laboratory experiments, we used magnetic properties to investigate the peak temperatures reached beneath a 40-cm-thick solidified portion of the June 27th Lava Flow (2014-2015) at Kīlauea Volcano. The control sample, from a site unaffected by the lava, had a weak initial magnetic susceptibility (~ 4×10^{-6} m^3kg^{-1}) at ambient temperatures, which increased fourfold after laboratory heating (Fig. 5a). In comparison, the initial susceptibility of sample MS3B from 5 cm beneath the lava was four times stronger and rose to a marked Hopkinson peak followed by a sudden drop indicating a Curie temperature of 580°C (Fig. 5b). This is characteristic behavior for fine-grained magnetite formed by intense heating (e.g. King and Ranganai 2001; Evans and Heller 2003; Butler 2004; Tauxe 2010; Dunlop 2014). Heating and cooling curves are reversible, showing that no further thermal alteration occurred during laboratory heating. Curves for sample MS3F from 23–25 cm beneath the lava flow fell between these two extremes. Some natural magnetic enhancement was evident, but the magnetic enhancement had not proceeded to an endpoint, since further enhancement took place during the laboratory heating. Consistent behaviour was seen in the NRM and demagnetisation of the samples. While the control did not carry any coherent magnetisation (Fig. 5c), the samples from beneath the lava all carried relatively strong, coherent remanent magnetisations with low inclinations. Their magnetisations were consistent with having been acquired during cooling in the geomagnetic field at the site at the time of eruption (From the International Geomagnetic Reference Field, the field direction at the site in 2014 had a declination of 9.6 and inclination of 35.9°; Thébault et al. 2015; Fig. 5d). The intensity of the NRM of the samples decreased with increasing depth below the flow, indicating a decreasing degree of magnetic enhancement, consistent with interpretation of the susceptibility vs temperature experiments. Further, the stability of the magnetisation, measured by the maximum coercivity and the median destructive field (field at which NRM is reduced by 50%), decreases with depth (Fig. 5e). This is also compatible with a profile of decreasing peak temperature with depth below the lava flow.

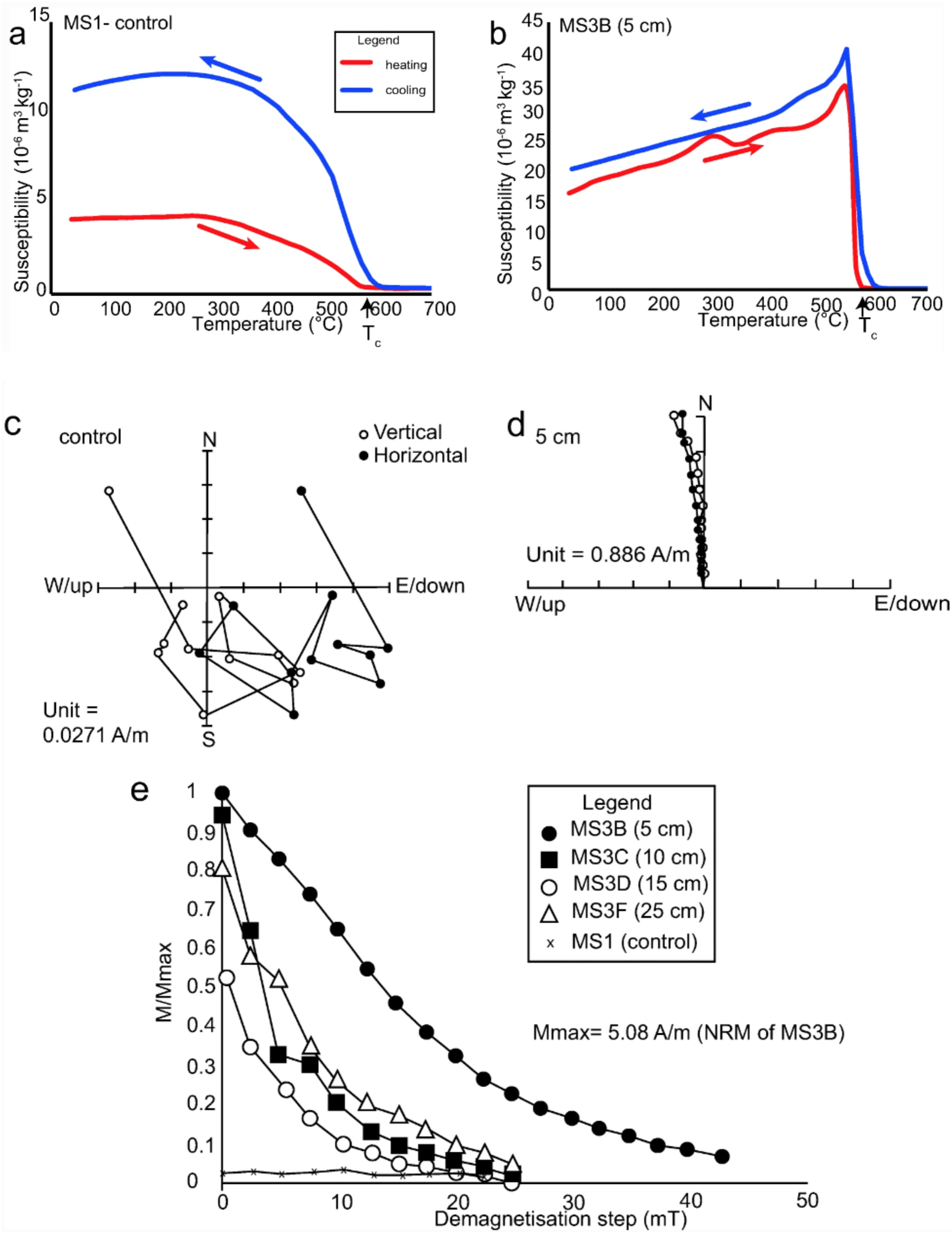

Fig. 5 a) and b) Variation of magnetic susceptibility with temperature on heating from room temperature to 700°C (red) and subsequent cooling (blue). c) and d) Vector component plots of data from progressive alternating field demagnetisation of the same samples. Solid black

symbols are the horizontal component (N vs. E) while open symbols are the vertical component (N vs. down) e) Progressive decrease of remanent intensity with alternating field demagnetisation for samples MS3B-F showing lower NRM intensity and stability with increasing depth below the lava flow. The control, MS1, is shown for comparison. All data have been normalised to Mmax, the NRM intensity of MS3B.

Heat transfer modelling

Our inputs are displayed in Tables 1–3, and model results are plotted in Fig. 4a (also see Online Resource 13). The experimental results in one of the 100 cm dry soil experiments is lower than those calculated by the model due to a thin crust of rock between the thermocouple and the molten rock. The crust formed while there was a fire in the sand pit. The fire temporarily suspended the molten rock pour while we extinguished it.

The heat transfer model was verified using the peak temperatures reached under the June 27th Lava Flow. To do so, we modelled a 40-cm-thick lobe of lava on dry soil. The lava temperature was set to 1150˚C based on the Kīlauea lava flow temperature data collected by Hon et al. (1993). The owner of the land on which this lobe was emplaced observed that the primary flow, to which this lobe was connected, was active for a week (M. Sugimoto *pers. comm.* (19/03/2017)). This is the only duration constraint available. The MAPDL modelling predicted that a two-day cooling duration was adequate for substrate temperatures to have fallen to below 100˚C after the cooling-only phase commenced. This duration agrees with our 50-cm dry substrate experiments. The heat transfer model calculated the peak temperature at 3 cm to be 788°C after 8 days and 50 minutes and was maintained for 1.9 hours. This is consistent with the palaeomagnetic data from 3–5 cm, which revealed the temperature should be above 580°C.

Applications of the heat transfer model

The heat transfer model enables quantitative estimates of heat transfer from lava flows, offering infrastructure providers the temperature profile estimates needed to make decisions.

For example, we have calculated the maximum temperature and depth of dry Auckland soil (Tables 1–3; Taihan New Zealand Ltd 2010; Atlas Concrete Ltd 2011; Rifareal 2011) that would be heated by a 2-m-thick lava flow that is active for four weeks (Table 4). In this scenario, no heat is removed from the sides of the lava flow (i.e. the sides are insulated). Although this assumption will lead to over-predictions, it can be justified because the centre of a lava flow would be well insulated by surrounding lava, especially in a wide flow. In the first week, 1.7 m of soil are heated to 100°C or above while 3.8 m of soil are hotter than 100°C after four weeks (Fig. 6). Such results suggest that water could boil and that electricity cables would be exposed to temperatures higher than standard operating temperatures (100°C, R. Joyce, *pers. comm.* (24/08/2017); Hawai'i County DWS, *pers. comm.* (19/04/2017)). These results represent an example output that can be tailored for a specific eruption and can be used in decision-making.

Table 4 Table showing the depth to which dry soil would be heated to 100 °C by a hypothetical lava flow for a given flowing phase duration, the total depth of substrate heated by the lava flow, and the maximum temperature reached in the soil. The lava flow was assumed to be a 2-m-thick pāhoehoe lava flow traversing dry Auckland soil.

Duration of flowing phase (weeks)	Depth of 100 °C contour at end of flowing phase (m)	Total depth of substrate heated (m)	Maximum temperature within 2.5 cm of lava-soil contact (Celsius)
1	1.7	3.1	695
2	2.3	4.8	775
3	3.2	6.5	851
4	3.8	7.6	885

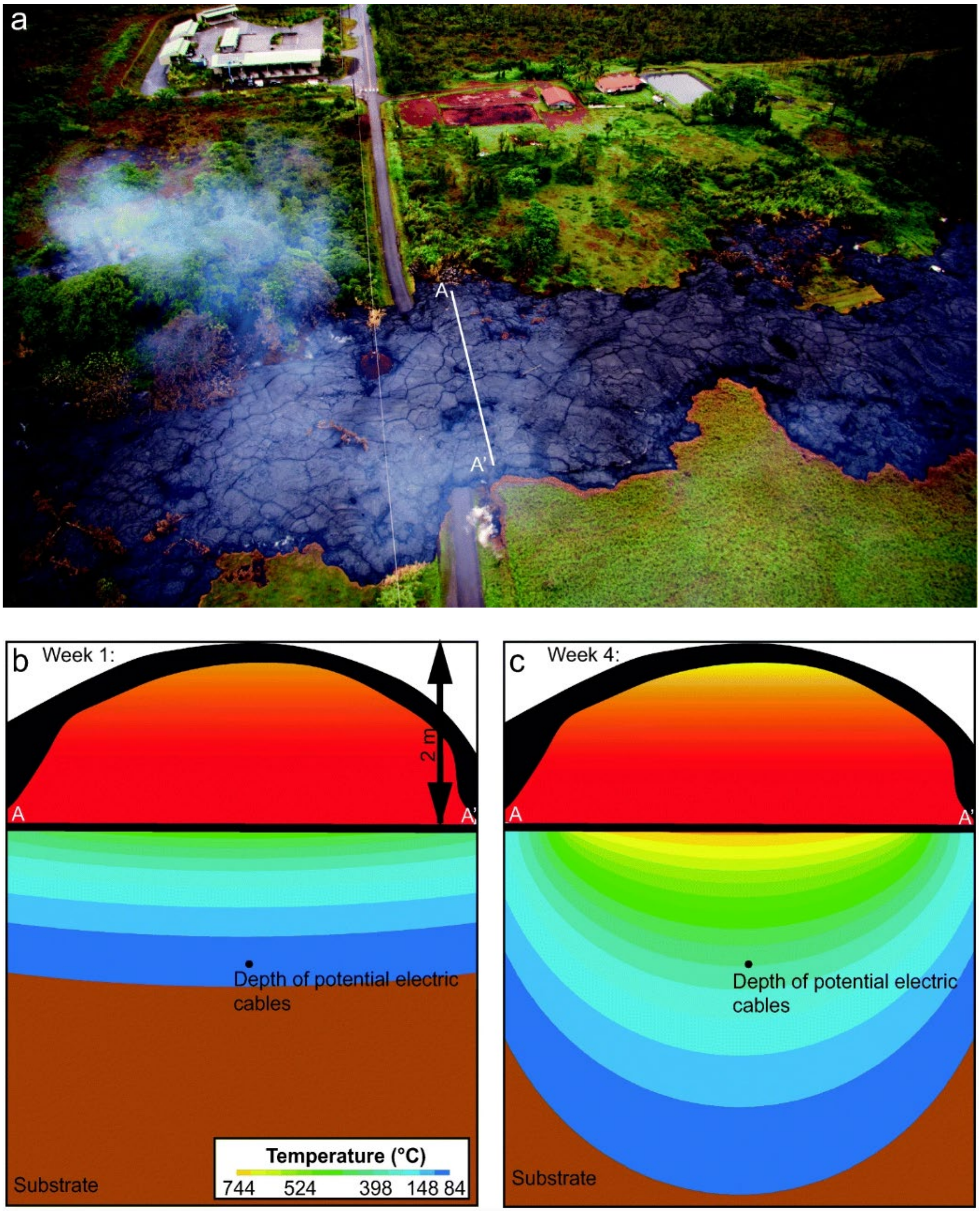

Fig. 6 a) Aerial photograph of the June 27th Lava Flow taken by the U. S. Geological Survey (public domain). Line AA' shows where the cross-sectional thermal profile was modelled. b) & c) The modelled temperature profile under a 2 m thick pāhoehoe lava flow after 1 and 4 weeks, respectively. Lava flow cross section shown for illustrative purposes, only. Lava flow crust growth not modelled.

Discussion

By collecting a suite of temperature profiles under cooling molten rock generated in laboratory experiments, it is possible to begin to infer the heat transfer mechanisms under lava flows. The initial temperatures at 20 cm below the molten rock-soil contact in the dry soil were warmer than those in the equivalent wet soil at corresponding times (Online Resource 2). This could be attributed to pore water boiling, as evidenced by the steam release at the beginning of the wet soil experiments. The formation of hydrothermal convection cells is possible, similar to those surrounding sills (Baker et al. 2015). Such convection cells could circulate heat more deeply over the course of the experiment and explain why the wet soil peak temperatures are warmer than the dry soil peak temperatures at corresponding depths (Fig. 4; Online Resources 1, 12, and 13). The wet soil results are likely more applicable to natural settings where the water table is close to the surface. The dry soil results could represent locations that are more arid and/or constrain the minimum limit on temperature increases in the substrates below lava flows.

In urban locations, the temperature profiles are altered by artificial ground coverings, which significantly alter the peak temperatures reached under the molten rock. The highest temperatures recorded in all the experiments were under the road ground covering in the base layer at 20 cm. This is likely due to the heat of combustion produced by the bitumen layer (the uppermost layer of the road) burning when the lava first made contact, as evidenced by the green smoke. Since a temperature spike was not measured below 20 cm, the heat likely diffused out of the pipe system in the base layer and did not cross the gravel-soil boundary efficiently due to the gravel's porosity.

It is important to consider the applicability of such analogue experiments to natural processes. This is especially important given the large differences between the temperature profiles from under the Kīlauea lava flow lobe and under the Lava Project molten rock experiments with similar lava thicknesses. The Kīlauea lava flow lobe transferred heat to the substrate for one week (M. Sugimoto, *pers. comm.* (19/03/2017)). In contrast, the analogue experiments were, active, for up to ten minutes and then cooled. This shows that the peak temperature is very strongly controlled by duration of the activity. Other factors influencing peak temperatures include where along the cross-sectional transect of the lava flow measurements are made, the thermal properties of the materials, weather conditions (Patrick et al. 2004), and the position of the water table (i.e. dryness of the substrate). While there are many factors that influence the peak temperatures under lava flows, a comparison of our experimental temperature profiles to the temperature profile under a lava flow emphasises the importance of the duration of the activity to model the heat transfer accurately.

We tried to control experimental factors to mimic the volcanic case as closely as possible. The temperature of the molten rock when it enters the pipes is important. Thus, the lava was heated above volcanic basaltic temperatures (i.e. to 1300°C; Dietterich et al. 2015) so it would be at suitable volcanic temperatures (i.e. 1200°C) when it entered the pipes (Online Resource 2). Lava flow thicknesses can vary with time (i.e. they can inflate; Hon et al. 1993), but the molten rock experiments were a constant thickness, which meant the heat transfer model also used a single thickness for all calculations. Additionally, not all lava flows display pāhoehoe morphotypes. As ʻaʻā lava flows currently cannot be made in a laboratory setting, more outcrops under ʻaʻā lava flows need to be identified and the underlying soil conditions thermally constrained to enable an ʻaʻā heat transfer model. This work provides a method to create such a heat transfer model. Alternatively, creating a laboratory methodology to simulate ʻaʻā lava flows would enable similar analogue experiments.

The coherence and strength of the magnetisation of the samples under the June 27th Lava Flow indicate that the remanent magnetisation in the soil was produced in a single cooling event from elevated temperatures. It is the strongest and most stable in the uppermost sample, with both strength and stability decreasing with depth (Fig. 5d and e). This indicates that deeper samples were heated to lower temperatures. Evidence for heating-induced magnetic enhancement also decreases with increasing depth, as displayed by the weakening trends of both magnetisation and susceptibility with depth (Fig. 5e). Taken together, magnetic susceptibility and remanence data suggest that the peak temperature was above the Curie temperature at a depth of 5 cm below the flow, with peak temperatures decreasing to possibly 200–300°C at 25 cm. The heat was sufficient to produce a significant (partial) TRM but not to complete the magnetic enhancement process. Better temperature estimates would be possible if a method were developed to prepare oriented soil samples for thermal demagnetisation treatment.

Conclusions

Natural lava flows are often thicker and active for longer durations than can be modelled in experiments necessitating field studies to supplement analogue studies. However, the heat transfer modelling presented in this paper represents a step towards defining the hazards posed to buried infrastructure in the path of lava flows. Our results suggest that many assets are likely buried deeply enough to continue functioning, at least during the beginning of an eruption, as heating to non-operable temperatures affects less than 2 m of the substrate over the first few days of heating. As the flow continues to be supplied with lava, the substrates continue to heat, possibly reaching conditions that would promote thermal erosion. Prior to a crisis, or after the initial onset of the eruption, the heat transfer model presented here could be run by stakeholders to determine how to best protect their systems.

Acknowledgements: We are grateful to Melvin and Ann Sugimoto and Wood Valley Coffee Planation for granting us land access to sample beneath the Hawaiian lava flows. We would like to thank Frank Trusdell, Bruce Hayward, and Peter Crossley for discussions and showing us field locations. We gratefully acknowledge Ryan McKay’s aid in implementing radiative heat transfer in ANSYS. We also greatly appreciate the thoughtful reviews of an anonymous reviewer and Elise Rumpf, which greatly improved the clarity of this manuscript. We would like to acknowledge Michael James and Andy Harris for their editorial handling. This work was funded by the New Zealand Earthquake Commission and was undertaken as part of the

Determining Volcanic Risk in Auckland (DEVORA) research programme. BK acknowledges support from "Quantifying exposure to specific and multiple volcanic hazards" program of the New Zealand Natural Hazards Research Platform (NHRP).

Author contributions

S.W.R.T. & J.M.L. conceived the study. S.W.R.T., R.W., & E.R. performed the molten rock experiments. S.W.R.T., G.A.L., & G.M.T. performed the palaeomagnetic analysis and interpretation. G.C. advised S.W.R.T. on the heat transfer modelling. J.M.L. & B.K. assisted S.W.R.T. in the field. All authors contributed to the preparation and editing of the manuscript.

References

Adams JA, Rogers DF (1973) Computer-aided heat transfer analysis. McGraw-Hill, New York, 426 p

ANSYS (2017) ANSYS Inc. PDF Documentation for Release 18.2. ANSYS Inc., Canonsburg, Pennsylvania, 43903 p

Arpaci VS, Kao S, Selamet A (1999) Introduction to heat transfer. Prentice Hall, Upper Saddle River, New Jersey, 611 p

As JA, Zijderveld JDA (1958) Magnetic cleaning of rocks in palaeomagnetic research. Geophys J R Astron Soc. 1: 308-319

Atlas Concrete Ltd (2011) Test results for Cable Trenching Pakuranga. Atlas Concrete Ltd, Takapuna, New Zealand, 7 p

Auckland Transport (2013a) Chapter 12: Footpaths and Pedestrian Facilities. In: Auckland Transport Code of Practice 2013. Auckland, Auckland Transport, 30 p

Auckland Transport (2013b) Road Pavement Drawing Index. Auckland, Auckland Transport, 7 p

Baker LL, Bernard A, Rember WC, et al. (2015) Temperature profile around a basaltic sill intruded into wet sediments. J Volcanol Geotherm Res. doi:

10.1016/j.jvolgeores.2015.06.012

Bell JF, Morris RV, Adams JB (1993) Thermally altered palagonitic tephra: A spectral and process analog to the soil and dust of Mars. J Geophys Res 98(E2): 3373–3385

Bergman TL, Lavine AS, Incropera FP, Dewit DP (2011) Fundamentals of Heat and Mass Transfer, 7th edn. Hoboken, New Jersey, John Wiley & Sons, 1048 p

Big Island Now (2018 May 6) Civil Defense Update on Leilani Estates Eruptions. Big Island Now. http://bigislandnow.com/2018/05/06/civil-defense-update-on-leilani-estates-eruptions/ Accessed 8 May 2018

Blong RJ (1984) Volcanic hazards: a sourcebook on the effects of eruptions. Sydney, Academic Press, 424 p

Bussey DBJ, Guest JE, Sorensen SA (1997) On the role of thermal conducivity on thermal erosion by lava. J Geophys Res 102:10905–10908

Bussey DBJ, Sorenson SA, Guest JE (1995) Factors influencing the capability of lava to erodie its substrate: Application to Venus. J Geophys Res 100:16941–16948

Butler RF (2004) Paleomagnetism: Magnetic domains to geologic terranes, Electronic edn. Portland, Oregon, University of Portland, 248 p

Chadima M, Hrouda F (2006) Remasoft 3.0 a user-friendly paleomagnetic data browser and analyzer. Travaux Geophysiques 27:20–21

Delaney PT (1987) Heat transfer during emplacement and cooling of mafic dykes. In: Halls HC, Fahring WF (eds.) Geological Association of Canada Special Paper 34. Geological Association of Canada, St John’s Newfoundland, pp 31–46

Delaney PT, Pollard DD (1982) Solidification of Basaltic Magma During Flow in a Dike. Am J Sci 282:856–885

Dietterich HR, Cashman KV, Rust AC, Lev E (2015) Diverting lava flows in the lab. Nat Geosci 8:494–496. doi: 10.1038/ngeo2470

Dunlop DJ (2014) High-temperature susceptibility of magnetitite: a new pseudo-single-domain effect. Geophys J Int 199: 707–716. doi: 10.1093/gji/ggu247

Edwards BR, Karson J, Wysocki R, et al. (2013) Insights on lava-ice/snow interactions from large-scale basaltic melt experiments. Geol 41:851–854. doi: 0.1130/G34305.1

Evans ME, Heller F, (2003) Environmental Magnetism. Academic Press, Sydney, 299 p

Fagents SA, Greeley R (2001) Factors influencing lava-substate heat transfer and implications for thermomechnical erosion. Bull Volcanol 62: 519–532. doi: 10.1007/s004450000113

Federal Highway Administration Research and Technology (2016) User Guidelines for Waste and Byproduct Materials in Pavement Construction. Federal Highway Administration. https://www.fhwa.dot.gov/publications/research/infrastructure/structures/97148/index.cfm. Accessed 10 October 2018

Goodhue R, Clayton G (2010) Palynomorph darkness index (PDI) - A new technique for assessing thermal maturity. Palynology 34:147–156. doi: 10.1080/01916121003696932

Greeley R, Fagents SA, Harris RS, Kadel SD, Williams DA, Guest JE (1998) Erosion by flowing lava: Field evidence. J Geophys Res Solid Earth 103(B11): 27325–27345. doi: 10.1029/97JB03543

Harris AJL (2015) Basaltic lava flow hazard. In: Shroder JF, Papale P (eds) Volcanic Hazards, Risks and Disasters. Elsevier, Waltham, MA, pp 14–46 doi: 10.1016/B978-0-12-396453-3.00002-2

Holman JP (2010) Heat Transfer, 10th ed. McGraw-Hill Higher Education, Boston, 725 p

Hon K, Kauahikaua JP, Mackay K (1993) Inflation and cooling data from pahoehoe sheet flows on Kilauea volcano. US Geological Survey. http://pubs.er.usgs.gov/publication/ofr93342A Accessed 5 August 2018

Hort M (1997) Cooling and crystallization in sheet-like magma bodies revisited. J Volcanol Geotherm Res 76: 297–317.

Ishihara K, Iguchi M, Kamo K (1989) Numerical simulation of lava flows on some volcanoes in Japan. In: Fink J (ed) Lava flows and Domes. IAVCEI, Berlin, pp 174–207 doi: 10.1007/978-3-642-74379-5_8

Jackson TA, Keller WD (1970) A comparative study of the role of lichens and “inorganic” processes in the chemical weathering of recent Hawaiian lava flows. Am J of Sci 269: 446–466.

Jaeger JC (1957) The Temperature in the Neighborhood of a Cooling Instrustive Sheet. Am J Sci 255:306–318.

Jenkins SF, Day S, Faria BVE, Fonesca JFBD (2017) Damage from lava flows: insights from the 2014-2015 eruption of Fogo, Cape Verde. J Appl Volcanol 6(1). doi: 10.1186/s13617-017-0057-6

Kauahikaua J, Cashman KV, Mattox TN, Heliker CC, Hon KA, Mangan MT, Thornber CR (1998) Observations on basaltic lava streams in tubes from Kilauea Volcano, island of Hawai’i. J Geophys Res Solid Earth 103(B11):27303–27323. doi: 10.1029/97JB03576

Kent DK, Ninkovich D, Pescatore T, Sparks R (1981) Palaeomagentic determination of emplacement temprature of Vesuvius AD 79 pyroclastic deposits. Nature 290: 393–396.

Kerr RC (2009) Thermal erosion of felsic ground by the laminar flow of a basaltic lava, with application to the Cave Basalt, Mount St. Helens, Washington. J Geophys Res Solid Earth 114(B9). doi: 10.1029/2009JB006430

Keszthelyi L (1995) Measurements of the cooling at the base of Pahoehoe Flows. Geophys Res Lett 22: 2195–2198. doi: 10.1029/95GL01812

Keszthelyi L, Denlinger R (1996) The initial cooling of pahoehoe flow lobes. Bull Volcanol 58: 5–18. doi: 10.1007/s004450050121

Keszthelyi L, Harris AJL, Dehn J (2003) Observations of the effect of wind on the cooling of active lava flows. Geophys Res Lett 30: 1–4. doi: 10.1029/2003GL017994

King JG, Ranganai RT (2001) Determination of magnetite grain-size using the Hopkinson effect- Examples from Botswana rocks. Botswana J Earth Sci 5: 35–38

Lerner GA, Cronin SJ, Turner GM, Piispa EJ (2019) Recognizing long-runout pyroclastic flow deposits using paleomagnetism of ash. Bull Geol Soc Am doi: 10.1130/B35029.1

Lev E, Spiegelman M, Wysocki RJ, Karson JA (2012) Investigating lava flow rheology using video analysis and numerical flow models. J Volcanol Geotherm Res 247–248: 62–73. doi: 10.1016/j.jvolgeores.2012.08.002

Lide DR (Ed.) (2005) CRC Handbook of Chemistry and Physics, 85th ed. CRC Press, Washington DC, 2656 p

Lovering TS (1935) Theory of Heat Conduction Applied to Geological Problems. Bull Geol Soc Am 46:69–94.

Lovering TS (1955) Temperatures in and near intrustions. Econ Geol 50th anniversary volume: 249-281.

Paterson GA, Roberts AP, Mac Noicaill C, Muxworthy AR, Guirioli L, Viramonte JG, Navarro C, Weider S (2010) Paleomagnetic determination of emplacement temperatures of pyroclastic deposits: an under-utilized tool. Bull Volcanol 72(3): 309–330. doi: 10.1007/s00445-009-0324-4

Patrick MR, Dehn J, Dehn K (2004) Numerical modeling of lava flow cooling applied to the 1997 Okmok eruption: Approach and analysis. J Geophys Res 109: 1–17. doi: 10.1029/2003JB002537

Patrick M, Orr T, Fisher G, et al (2017) Thermal mapping of a pāhoehoe lava flow, Kīlauea Volcano. J Volcanol Geotherm Res 332: 71–87. doi: 10.1016/j.jvolgeores.2016.12.007

Reilly WI (1958) Temperature distribution about a cooling volcanic intrusion. NZ J Geol Geophys 1:364–374. doi: 10.1080/00288306.1958.10423188

Rifareal RL (2011) North Island Upgrade Project Brownhill Rd to Pakuranga- Design, Supply and Install 220 kV Underground Cables. Taihan New Zealand Ltd, Auckland, NZ, 9 p

Rumpf ME (2015) Lava-Substrate Heat Transfer: Implications for the Preservation of Volatiles in the Lunar Regolith. Dissertation, University of Hawaii- Manoa

Rumpf ME, Fagents SA, Crawford IA, Joy KH (2013) Numerical modeling of lava-regolith heat transfer on the Moon and implications for the preservation of implanted volatiles. J Geophys Res Planets 118: 382–397. doi:10.1029/2012JE004131

Rumpf ME, Lev E, Wysocki R (2018) The influence of topographic roughness on lava flow emplacement. Bull Volcanol 80. doi:10.1007/s00445-018-1238-9

Stretch RC, Viles HA (2002) The nature and rate of weathering by lichens on lava flows on Lanzarote. Geomorphology 47: 87–94.

Taihan New Zealand Ltd. (2010) Thermal Resistivity Testing. Transpower, Auckland NZ, 26 p

Tauxe L, (2010) Essentials of Paleomagnetism. University of California Press, Berkeley, California, 490 p

Thébault E, Finlay CC, Beggan CD et al. (2015) International Geomagnetic Reference Field: the 12th generation. Earth, Planets, and Space 67. doi: 10.1186/s40623-015-0228-9

Thompson R, Bloemendal J, Dearing JA, Oldfield F, Rummery TA, Stober JC, Turner GM (1980) Environmental applications of magnetic measurements. Sci 207: 481–486

Trusdell FA, Wolfe EW, Morris J (2006) Digital Database of the Geologic Map of the Island of Hawai'i. US Geological Survey. https://pubs.usgs.gov/ds/2005/144/ Accessed 15 August 2018

Turner GM, Alloway BV, Dixon BJ, Atkins C (2018) Palaeomagnetic interpretation of the thermal history of mass-flow deposits on the eastern flanks of Mt Taranaki/Egmont Volcano, New Zealand: implications for linkage to known eruptive events and future hazards. J Volcanol Geotherm Res 353: 55–67

Wilson RL (1962) The Palaeomagnetism of Baked Contact Rocks and Reversals of the Earth's Magnetic Field. Geophys J R Astron Soc 7:194–202

Wirth KR, Vervoort JD, Naiman ZJ (1997) The Chengwatana Volcanics, Wisconsin and Minnesota: petrogenesis of the southernmost volcanic rocks exposed in the Midcontinent rift. Can J Earth Sci 34: 536–548. doi: 10.1139/e17-043

Zicar Ceramics (2016) Alumina Mat Alumina Mat. Zicar Ceramics, Inc, Florida NY, 2 p

Online Resources:

Online Resource 1: Full data tables and graphs.

Online Resource 2: Table of molten rock temperatures derived from the thermal camera and the data loggers.

Online Resources 3—11: Videos of molten rock experiments.

Online Resource 12: Maximum temperatures reached at the given depths in the model results and the corresponding experiments. The time (in hours) that the substrate reached the maximum temperature is provided in parentheses.

Online Resource 13: Summary table of substrate temperature data over time from the Lava Project experiments and the corresponding modelling. The experimental data shown is from the experiment on which the model was based. See Online Resource 1 for extended data.